Leveraging mmWave for Contactless Breath Rate Estimation of Moving Subjects

Cristian Turetta
Department of Computer Science
University of Verona
Verona, Italy
cristian.turetta@univr.it

Morteza Varasteh
School of Computer Science and Electronic Engineering
University of Essex
Colchester, United Kingdom
m.varasteh@essex.ac.uk

Şefki Kolozali
School of Computer Science and Electronic Engineering
University of Essex
Colchester, United Kingdom
sefki.kolozali@essex.ac.uk

Graziano Pravadelli
Department of Engineering for Innovation Medicine
University of Verona
Verona, Italy
graziano.pravadelli@univr.it

***Abstract*—The breath rate (BR) measurement is fundamental for comprehensive human health monitoring in many scenarios. Accurately estimating BR, particularly in moving subjects, poses several challenges, including the necessity for direct physical contact with the individual or constraints on the individual's movements and mobility. In this paper, a methodology is proposed that employs frequency-modulated continuous wave (FMCW) radar, operating at a frequency of 77 GHz, to estimate the BR of subjects moving freely within an environment. The proposed methodology features a pre-processing pipeline designed to refine the radar's captured signals. The processed signals are used to accurately track the subject, and estimate their corresponding BR. Preliminary outcomes of our investigation indicate that the BR estimates generated by our system exhibit a mean absolute error (MAE) of 2.48 breaths per minute, as averaged across four subjects when compared with the ground truth.**

***Index Terms*—Contactless breath rate monitoring, Millimeter-wave, Radar technology, Indoor monitoring.**

I. Introduction

Breath rate (BR) monitoring is essential to evaluating an individual's physiological condition across numerous applications, from clinical diagnostics to athletic performance and home healthcare [1]. Historically, BR measurement has relied mainly on direct contact methods, such as spirometry, chest straps, face masks, and nasal prongs [2], [3]. These methods, although accurate, often hinder the subject's natural activities due to their intrusive nature [4], besides the limitations due to the battery life, connection with a companion device, et cetera. The evolution of monitoring technologies has been directed increasingly towards minimizing patient discomfort and maximizing non-intrusive observation of physiological parameters. This trend has catalyzed the development of contactless measurement techniques, mainly using radio-based sensing technologies [5]–[7]. Among these, millimeter-wave (mmWave) radar-based systems have opened a new perspective to address the aforementioned challenges. These systems use frequency-modulated continuous wave (FMCW) radar operating typically in high-frequency bands (e.g., 77-81 GHz), thus allowing FMCW radars to detect tiny movements, such as those associated with human respiration. This capability addresses a notable gap in health monitoring practices, unlocking the ability to measure physiological metrics in a non-intrusive way, accurately.

This paper has been supported by the "UNISCO" project (CUP: 1695-0026-553-2023) - PR Veneto FSE+ 2021-2027 and the PRIN 2022 project "WE.SMOOTH.PD: a WEarable-based System to MOnitor motor functions and levodopa levels for THerapy optimization in Parkinson's Disease" (code: 2022EJM345)

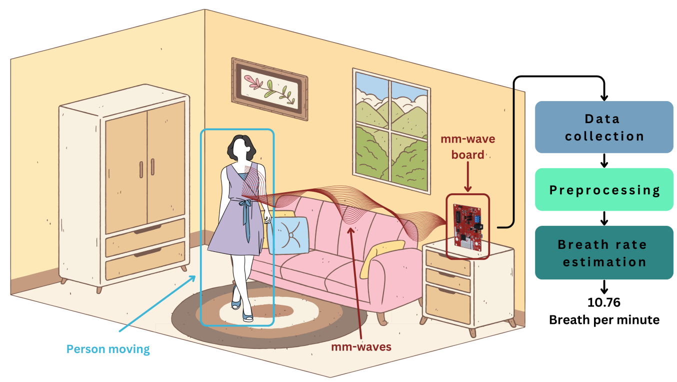

Fig. 1: Overview of the breath rate estimation system.

Several notable studies have contributed to the advancement of contactless vital sign estimation. Yang et al. [8] introduced the *mmVital* system, which utilizes 60GHz mmWave signals to monitor vital signs such as breathing and heart rates with high accuracy. Ahmad et al. [9] proposed an FMCW based radar system for simultaneous monitoring of multiple individuals, overcoming challenges surrounding clutter pose. Liu et al. [10] developed a method for detecting heart and breathing rates using a 77GHz mmWave radar sensor, employing a coarse-to-fine estimation approach to mitigate the impact of breathing harmonics. Furthermore, Liu et al. [11] presented a framework for vital sign estimation during random body movements in stationary positions, enabling monitoring in dynamic scenarios where traditional static methods are impractical. Wang et al. [12] proposed an integrated system combining mmWave radar and camera technologies to monitor vital signs in dynamic environments, achieving high accuracy even in the presence of subject movement. Despite these advancements, existing techniques often require subjects to remain stationary or sleep-like, limiting their applicability in real-world scenarios where movement is unavoidable.

To overcome this limitation, in this preliminary study, we introduce a novel methodology for estimating breath rate in moving subjects using processed mmWave radar data, as depicted in Figure 1. Unlike existing approaches, our method does not rely on a stationary subject, thereby expanding the applicability of contactless vital sign monitoring to dynamic environments. The main contribution of this paper includes:

- A signal processing pipeline to detect, track, filter, and compensate the data of the subject moving in the environment.
- A breath rate estimation technique combining two approaches based on time and frequency domain data analysis.
- An extensive evaluation of the proposed methodology on four subjects in a real-world unconstrained home environment.

By enabling accurate vital sign monitoring in dynamic environments, our work contributes to advancing contactless healthcare technology and opens new possibilities for continuous health monitoring in everyday settings. The remainder of this paper is organised as follows: In Section II, the preliminary background is provided, followed by a detailed description of our methodology in Section III, focusing on technical details. The experimental results are presented in Section IV, while in Section V we review related works. Finally, in Section VI, we conclude and discuss future extensions of our work.

II. Preliminaries

Millimeter-wave radar systems are pivotal in modern sensing applications, offering precise estimation of distance, velocity, and direction of multiple targets. These systems operate by emitting radar waves that are reflected off objects and return to the radar. Analysis of these reflected signals enable the estimation of various parameters essential for autonomous vehicle navigation, traffic monitoring, and similar applications.

Round-Trip Time Delay Estimation

The primary function of mmWave radar involves the measurement of the time delay between the transmission and reception of the radar signal. This time delay, indicative of the distance to the target, is calculated using the equation:

$$x(t) = \alpha s(t - \tau) + w(t), \tag{1}$$

where $x(t)$ is the received signal, α represents the attenuation, $s(t)$ is the transmitted signal, τ is the time delay, and $w(t)$ is additive white Gaussian noise. The matched filter output for maximizing the signal-to-noise ratio (SNR) is:

$$y(\tau) = \int x(t) s^*(t - \tau) dt, \tag{2}$$

and the time delay τ is estimated by the maximum likelihood method:

$$\hat{\tau} = \arg\max_{\tau} |y(\tau)|. \tag{3}$$

Target Detection

The capability to detect and distinguish multiple targets simultaneously is facilitated through FMCW radar. The FMCW radar enhances detection capabilities by transmitting a signal that varies in frequency over time. In the following, we neglect the effects of Gaussian noise $w(t)$ and attenuation α. We have

$$s(t) = e^{j2\pi\left(f_c + \frac{S}{2}t\right)t} \quad \text{for } 0 \le t \le T, \tag{4}$$

where f_c is the carrier frequency and $S = \frac{B}{T}$ is the slope of the chirp signal $s(t)$[1]. A mixer[2] combines the transmitted and received signals to produce an intermediate frequency (IF) signal. The IF signal can be expressed as

$$\begin{aligned} r_{\text{IF}}(t) &= e^{j2\pi\left(f_c + \frac{S}{2}t\right)t} \cdot e^{-j2\pi\left(f_c + \frac{S}{2}(t-\tau)\right)(t-\tau)} \\ &= e^{j2\pi F(t)}. \end{aligned} \tag{5}$$

Focusing on $F(t)$ in (5), we have

$$\begin{aligned} F(t) &= \left(f_c + \frac{S}{2}t\right)t - \left(f_c + \frac{S}{2}(t-\tau)\right)(t-\tau) && (6)\\ &= S\tau t + f_c t - \frac{1}{2}S\tau^2 && (7)\\ &= f_b t + f_c\tau - \frac{1}{2}f_b\tau, && (8) \end{aligned}$$

where $f_b = S\tau$. Note that

$$\tau = \frac{2(vt + d) + l\sin\theta}{c} \tag{9}$$

with v, d and θ being the relative velocity, distance and angle of an object to the antenna. Additionally, c represents the speed of light. Substituting (9) in (8) we have:

$$\begin{aligned} F(t) =& f_b t + \frac{2df_c}{c} + \frac{2vtf_c}{c} + \frac{l\sin\theta f_c}{c} \\ & - \frac{df_b}{c} - \frac{vtf_b}{c} - \frac{l\sin\theta f_b}{2c} && (10)\\ \approx& f_b t + \frac{2df_c}{c} + \frac{2vtf_c}{c} + \frac{l\sin\theta f_c}{c}, && (11) \end{aligned}$$

where (11) is due to the fact that the second line of (10) is negligible.

The output of the mixer is sampled every T_s seconds. Since the signal is repeated every T seconds, each sample can be attributed with a time $t = pT + nT_s$ for some integer $0 \le p \le$

[1]The slope refers to the rate at which the signal's frequency changes over time, expressed in units of frequency per unit time. Here, B represents the bandwidth, and T is the duration of the transmitted signal.

[2]A frequency mixer is an electronic component that combines two signals to produce a new signal at a different frequency.

N_{Ch} and $0 \leq n \leq N_{\text{ADC}}$[3]. Thus, considering that $pTf_b = 2\pi k$ for some integer k, and defining $f_d = \frac{2cf_c}{c}$, the sampled $F(t)$ can be expressed as

$$F(pT + nT_s) = \frac{2df_c}{c} + \frac{l \sin\theta f_c}{c} + nT_s(f_d + f_b) + pTf_d. \quad (12)$$

Note that the first FFT, known as the *range FFT*, is performed across the ADC samples (fast sampling) which is used to extract $f_d + f_b$. This frequency component is crucial for localizing objects, i.e., estimating the distance of objects relative to the radar. The second FFT, referred to as the *range-Doppler FFT*, is carried out across the chirps in a frame (slow sampling) and extracts the frequency f_d, which is employed to estimate the velocity of the objects. The third FFT is implemented across the antennas and is used to estimate the angular location of objects relative to an FMCW radar. For a detailed understanding of the full operation of a mmWave radar system, we refer the reader to [13], [14].

III. Methodology

Figure 2 depicts an overview of the proposed methodology. It comprises six phases, starting from the data collection to the breath rate estimation. This section provides details of each phase.

A. Data collection setup

Our data collection setup employed the Texas Instruments (TI) AWR1243 BOOST mmWave board [15]. This board interfaces with the DCA 1000 EVM from Texas Instruments, allowing real-time data streaming from the mmWave board to a computer. The orchestration of data flow and capture settings relies on the mmWave Studio software provided by TI. In particular, to detect the breath rate of moving subjects, we set the mmWave board as reported in Table I. We used one transmitting antenna (`Tx`) and one receiving antenna (`Rx`) with a measurement rate of 70 Hz, 374 samples per chirp and 99 chirp loops.

In order to simulate realistic conditions and evaluate the performance of our breath rate estimation system, we gathered data from one subject at a time, moving freely within an environment. This approach was necessary for assessing the system's robustness and accuracy in dynamic scenarios, closely mimicking real-world applications. A total of four subjects participated in this data collection. Each recording lasted 2.40 minutes of continuous data collection, providing a uniform duration across all participants.

B. Preprocessing pipeline

Estimating breath features from the FMCW can be challenging, and environmental and movement conditions heavily affect the results. For this reason, the collected data undergoes the following preprocessing steps.

[3]Note that each FMCW signal constitutes a frame composed of chirps. N_{Ch} denotes the number of chirps per frame, and N_{ADC} denotes the number of samples per chirp. It is worth mentioning that in the literature, the concepts of slow sampling and fast sampling relate to T and T_s, respectively.

TABLE I: Hardware and sensing settings used for breath rate estimation.

Sensing settings	
Hardware	Texas Instruments AWR1243
Tx antennas	1
Tx power	12 dBm
Rx antennas	1
Bandwidth	77-81 GHz
Max Bandwidth	4 GHz
Chirp slope	3.013×10^{13}
ADC sample rate	3×10^6
Samples per chirp	374
# chirp loops	99
Measurement rate	70 Hz

1) Range FFT: The Analog-to-Digital Converter (ADC) converts raw analog signals into a digital format. The converted digital signal, which carries information about the reflected electromagnetic waves, is referred to as *ADC data*. The Range Fast Fourier Transform (RFFT) application is the first step in processing these ADC data. The RFFT transforms data from the time domain to the frequency domain. When applied to the ADC data of a reflected signal, the RFFT breaks the signal down into its constituent frequency components. These frequency components that exhibit significantly distinct amplitudes, compared to others, correspond to different objects in the environment. When a person is stationary, the frequency component $f_d + f_b$ in (12) remains approximately unchanged over time. Therefore, to detect chest movement, one needs to filter the received signal at this frequency and extract the phase change over time. This data can then be used to estimate the movement of the subject's chest, leading to the detection and estimation of the breathing rate. However, the main challenge arises when the subject is moving.

For a moving object, it is essential to monitor the object frequency bin obtained from RFFT over ADC samples of a chirp in real-time. This task becomes even more challenging when multiple objects, indistinguishable from humans, create interference. Such interference occurs when their relative distances to the radar are the same, causing all these objects to fall within the same frequency bin upon applying RFFT. Once appropriate tracking mechanisms (tracking and filtering) are in place, the system can proceed as before, i.e., extracting the signal's phase over time to detect and estimate chest movement, which, as a byproduct, determines the breathing rate.

2) Subject detection: Detecting and tracking subjects in a cluttered environment, such as when multiple static objects (e.g., furniture) indistinguishable from humans are present, poses a significant challenge. Our approach leverages sliding window analysis across consecutive radar frames to address this challenge. This technique is critical for distinguishing between the subject's movements, which may be small yet consistent if the subject is still breathing, and the permanent positions of surrounding objects.

The sliding window method involves the subtraction of two

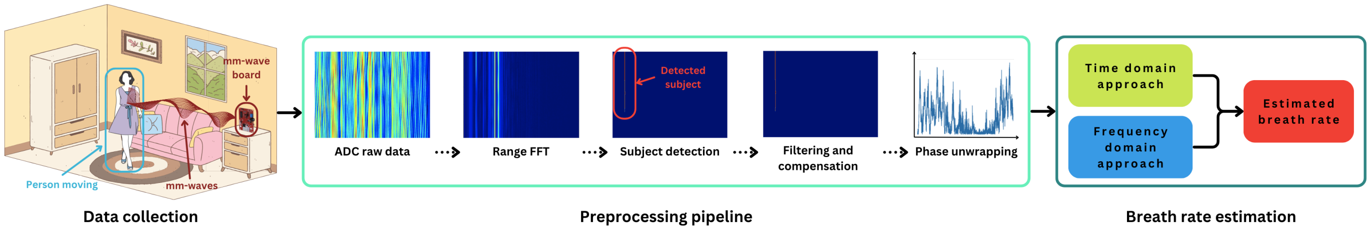

Fig. 2: Methodology overview.

consecutive data segments (windows) that move frame by frame across the obtained RFFT data. The differences between two consecutive frame highlight the range variations (subject) from constant ranges (objects). The result of this phase is map of peaks locations, related to the subject, in the frame.

3) Filtering and compensation: In order to remove possible outliers from the peaks related to the subject, we adopt a clustering technique. This technique clusters peaks based on their proximity to other peaks within each frame of RFFT, retaining only those with significant corroborative evidence. Specifically, to be considered a valid cluster, it has to contain at least five peaks within a spatial range of 5 RFFT bins[4]. This approach helps to mitigate the influence of random noise or transient signals that do not represent the subject. Peaks that do not meet this criterion are classified as outliers and excluded.

Furthermore, we apply range compensation on the RFFT clusterized peaks data to filter out noise carried by other body movements (e.g., walking or minor gestures). This compensation works by dynamically adjusting the RFFT analysis to the specific range bins that are likely influenced by respiratory motion. It takes into account the variability in distance caused by movements of the subject, which might otherwise lead to errors in detecting the true respiratory frequency. For each clusterized peak in the frame, the compensation is calculated as follows:

$$\text{compensation}_i = e^{-2\pi j \cdot \frac{f_i}{F_{adc}}} \tag{13}$$

where f_i is the frequency bin of the i^{th}-peak and F_{adc} is the ADC sample rate (in this case 3×10^6). The compensation is then multiplied to the respective peak value.

4) Phase unwrapping: At this stage, we extract the phase values of signals collected across different RFFT bins. Since the collected phase from different RFFT bins is wrapped, every time the phase exceeds π or $-\pi$, the phase wraps around to the opposite end of the scale. This results in discontinuities in the collected phase over time. The phase unwrapping process corrects these discontinuities, ensuring a continuous phase signal that accurately reflects the changes over space (across different RFFT bins) and time (across different frames). Analyzing the differences between adjacent phase values, when it exceeds the threshold $\pm\pi$, we adjust the phase by adding or subtracting 2π accordingly.

[4]The choice of 5 peaks is according to multiple experiments.

C. Breath rate estimation

We leverage the combination of two approaches to estimate the breath rate from the reprocessed data. Specifically, we perform the estimation using both time domain and frequency domain based approaches simultaneously. The outputs of these two methods are ultimately merged by averaging the produced results. The details of these two approaches are as follows.

1) Time domain approach: In this approach, the estimation process begins with calculating the differential of the unwrapped phase data. This differentiation helps to highlight changes in the phase signal corresponding to the chest's movement during respiration. By focusing on these changes rather than the absolute phase values, we can improve the detection of breathing patterns.

Following the differentiation of the phase, the next step involves applying a band-pass filter to the resultant phase difference signal. This filtering step is designed to eliminate high-frequency noise that does not correspond to human respiration, thereby refining the signal to include only the frequencies within the typical respiratory range of approximately 0.16 to 0.50 Hz [16]. We selected these frequencies based on respiratory rates for adults, which typically fall between 10 and 30 breaths per minute.

Peak identification is the next step after band-pass filtering. These peaks are indicative of individual respiration cycles. In our method, peak detection is crucial as each peak corresponds to a specific point in the breathing cycle, typically the maximum inhalation or exhalation. Accurately identifying these peaks is essential for determining the rhythm and rate of respiration.

The final step in our breath rate estimation process is calculating the time difference between consecutive peaks in the filtered phase difference signal. This time difference represents the period of the respiration cycle. By measuring the interval between peaks, we can directly compute the frequency of respiration, which is inversely proportional to the period. This method allows us to convert the time intervals between breathing peaks into a quantitative measure of breath rate per minute, providing a direct and effective metric for assessing respiratory function.

2) Frequency domain approach: In this approach, we exploit the Short-Time Fourier Transform (STFT). The STFT is applied to transform the data from the time domain into the frequency domain, segment by segment, allowing us to observe how frequency components evolve over time. This transformation is crucial as it clearly depicts the periodic nature of breathing within the collected data.

We employ a Hamming window in the STFT calculation to reduce spectral leakage, which can blur the distinction between closely spaced frequency components. The length of each segment for the Fourier transform is chosen to be 256 points, balancing the need for sufficient frequency resolution with computational efficiency. Once the STFT is applied, the result is a complex matrix representing the spectrum at various points in time. Our analysis focuses on the lower frequencies, specifically the first five frequency bins of the STFT output, which correspond to the same frequency range utilized in Section III-C1. We then calculate the average spectral magnitude across all time frames to condense the data into a single spectrum representing the dominant frequencies throughout the recording period.

To identify significant respiratory cycles, we detect peaks in this averaged spectrum. These peaks indicate the presence of strong periodic components that are likely related to the subject's breathing, ensuring that only the most prominent frequencies are considered for further analysis.

After identifying these peaks, the next step involves calculating the breath rate. For each detected peak in the frequency domain, we determine the corresponding frequency. This frequency is then converted into breaths per minute. If multiple peaks are detected, we average the results to obtain a single breath rate value, providing a more stable and reliable estimate.

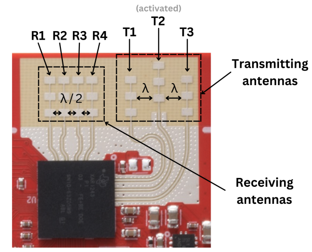

(a) Texas Instruments AWR1243 antennas characteristics and geometry.

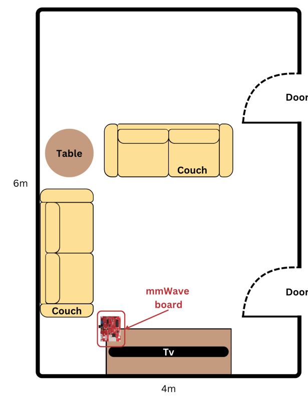

(b) Data collection environment. The mmWave board is in portrait position, facing the room.

Fig. 3: Data collection environment and antenna setup.

IV. Experimental results

This section investigates the results of the proposed methodology via experimental implementations and observations. The primary objective is to estimate the performance of the breath rate estimation algorithm on different subjects roaming inside an unconstrained house environment.

A. Data collection

To gather the data for the evaluation of the proposed methodology, as reported in Section III, we employed the TI AWR1243 radar, depicted in Figure 3a, operating at 77-81 GHz. The settings used are listed in Table I for all experiments. The data collection took place in an unconstrained house environment. The AWR1243 radar was placed at 30 cm height on top of the television stand, as shown in Figure 3b. During the recording, only one subject was present in the environment, and he/she was free to roam around without constraints, such as prescribed paths, specific distances from the radar, angle of view, or body orientation. The data collection involved 4 volunteers (2 male and 2 female), who were free to breathe normally.

Ground truth data for breath rate was meticulously collected to ensure accuracy and reliability. During the data collection sessions, the subjects were counting their breaths. At the same time, an Apple Watch Series 8 was gathering subjects' breath rates, thus providing a digital measurement of respiratory frequency. Each experimental recording is accurate and suitable to validate our methodology only if the breath count reported by the subject matches the rate recorded by the Apple Watch, allowing for a marginal error of ± 2 breaths. Thus, this method ensures that the counts provided by the subjects are sound and can be considered ground truth data. We note that all the subjects were free from respiratory, cardiac, or any other diseases that may alter the outcome of this paper.

B. Breath rate estimation results

To measure the performance of our breath rate estimation algorithm, we exploit the Mean Absolute Error (MAE) as a performance metric, ideally to measure the accuracy of continuous variables like breath rate [17], [18]. The MAE formula used is defined as follows:

$$\text{MAE} = |BrPM_{gt} - BrPM_{est}| \tag{14}$$

where $BrPM_{gt}$ is the ground truth breath rate, while $BrPM_{est}$ is the estimated breath rate, both expressed in breaths per minute (BrPM). Table II presents the results obtained from the proposed methodology. We performed several tests on different time window sizes to find the best configuration for our algorithm. As a result, we obtained the best performance using a time window of 35 seconds, resulting in an MAE of 2.48 (highlighted in green on Table II). Furthermore, we noticed that the estimation cannot be calculated on time windows small time windows (e.g., 1 second). The

TABLE II: Results of breath rate estimation in Breaths per Minute (BrPM)

Subject	**Ground truth**	**15 sec window**		**30 sec window**		**35 sec window**		**40 sec window**		**70 sec window**	
		Estimated	*MAE*	*Estimated*	*MAE*	*Estimated*	*MAE*	*Estimated*	*MAE*	*Estimated*	*MAE*
S0 session 1	5.03	5.31	0.28	7.18	2.15	6.91	1.88	6.83	1.80	6.43	1.4
S1 session 1	15.10	5.76	9.34	6.07	9.03	11.45	3.65	6.85	8.25	11.4	3.7
S2	11.33	3.72	7.61	8.62	2.71	10.76	0.57	14.1	2.77	4.32	7.01
S3	6.29	5.13	1.16	2.92	3.37	4.90	1.39	5.72	0.57	7.06	0.77
S0 session 2	6.29	8.60	2.31	11.5	5.21	5.40	0.89	3.82	2.47	4.38	1.91
S1 session 2	11.33	7.52	3.81	5.27	6.06	4.81	6.52	5.78	5.55	6.96	4.37
Average	-	-	4.08	-	4.76	-	2.48	-	3.57	-	3.19

results indicate that the breath rate estimation for four out of six subjects achieve optimal results getting a MAE of ≤ 1.9 BrPM.

V. Related Work

Recently, several works related to contactless vital sign estimation have been proposed. In [8], authors present the mmVital system, which utilizes 60GHz mmWave signals for non-contact monitoring of vital signs like breathing and heart rates. This system can accurately estimate these vital signs by directing mmWave signals at the human body and analyzing the reflections' received signal strength (RSS). Additionally, mmVital supports sleep monitoring, identifying sleep postures, and detecting central apnea and hypopnea events. The system demonstrated a mean estimation error of 0.43 breaths per minute for breathing rate and 2.15 beats per minute for heart rate.

Authors in [9] use an FMCW radar sensor for non-contact monitoring of vital signs in multiple individuals simultaneously. Their system leverages the range-gating ability of FMCW waveforms along with multiple receive channels to differentiate objects in the range-azimuth plane. Thus, they applied techniques like range-gating and beamforming to isolate breath and heart rate from surrounding clutter.

The work proposed in [10] introduces a system for detecting heart and breathing rates using a 77GHz mmWave radar sensor. The method focuses on the phase changes of the FMCW radar signal, which are influenced by the physiological movements. The study develops a coarse-to-fine estimation approach to address the challenge of breathing harmonics impacting the heart rate spectrum. Initially, it predicts the heart/breath rate from the unwrapped phase signal in the time domain, applying an adaptive threshold to filter out invalid peak-valley pairs. Subsequently, the heart/breath rate is estimated in the spectral domain, refining the initial prediction.

In [11], authors introduce a comprehensive framework to detect and estimate heart and respiration rates when subjects are engaged in random body movements. This method is tested in scenarios where traditional static vital sign monitoring is not feasible, such as in dynamic environments or when subjects use devices like laptops.

The work proposed by authors in [12] proposes a non-contact vital sign monitoring system that integrates mmWave radar and camera technologies to function effectively in dynamic environments. The integration aids in overcoming inaccuracies caused by subject movement and environmental changes. The system employs a camera to locate subjects accurately, uses beamforming to enhance radar signal reception, and applies a novel Weighted Multi-Channel Variational Mode Decomposition (WMC-VMD) algorithm to effectively distinguish vital signs from dynamic movements. Experimental results showcase high accuracy, with 90th percentile errors under 0.5 BPM for respiration and less than 6 BPM for heart rates, proving the system's efficacy in environments with significant movement.

In summary, in the state-of-the-art, the majority of the works propose heart/breath rate estimation with a significant limitation: the subjects need to stay still or sleep. Recent works like [11], [12] addressed the challenges of random body movements in a stationary position, such as typing on a laptop while seated or performing data fusion with video cameras to estimate vital signs in moving subjects. On the other hand, the proposed work provides a methodology to estimate the breath rate on a moving subject just by using mmWave radar data.

VI. Conclusions and Future Work

The paper presents a methodology that exploits FMCW radar to estimate the breath rate of a moving subject within an environment. We tested the proposed methodology on four subjects, achieving, in the worst-case scenario, a MAE of 6.52 BrPM, while the average MAE was 2.48 BrPM. These results are considered acceptable when compared to the state-of-the-art, where achieving precise results often imposes significant constraints on the subject.

In future work, we plan to enhance the estimation capabilities of our system by adding heart rate estimation. Furthermore, we intend to extensively test the methodology on a broader number of subjects engaged in specific activities to provide deep insights into how different activities affect the radar data and the consequent impact on the accuracy of vital signs estimation. This process will be facilitated by employing fine-grained ground truth data collected from wearable sensors to precisely log both heart and breath rates.

References

[1] A. Nicolò, C. Massaroni *et al.*, "The importance of respiratory rate monitoring: From healthcare to sport and exercise," *Sensors*, vol. 20, no. 21, p. 6396, 2020.

[2] J. Kranjec, S. Beguš *et al.*, "Non-contact heart rate and heart rate variability measurements: A review," *Biomedical signal processing and control*, vol. 13, pp. 102–112, 2014.

[3] T. Hussain, S. Ullah *et al.*, "Wearable sensors for respiration monitoring: A review," *Sensors*, vol. 23, no. 17, p. 7518, 2023.
[4] H. C. Bidsorkhi, N. Faramarzi *et al.*, "Wearable graphene-based smart face mask for real-time human respiration monitoring," *Materials & Design*, vol. 230, p. 111970, 2023.
[5] G. Paterniani, D. Sgreccia *et al.*, "Radar-based monitoring of vital signs: A tutorial overview," *Proceedings of the IEEE*, 2023.
[6] S. Ahmed and S. H. Cho, "Machine learning for healthcare radars: Recent progresses in human vital sign measurement and activity recognition," *IEEE Communications Surveys & Tutorials*, 2023.
[7] R. Shahbazian and I. Trubitsyna, "Human sensing by using radio frequency signals: A survey on occupancy and activity detection," *IEEE Access*, 2023.
[8] Z. Yang, P. H. Pathak *et al.*, "Vital sign and sleep monitoring using millimeter wave," *ACM Transactions on Sensor Networks (TOSN)*, vol. 13, no. 2, pp. 1–32, 2017.
[9] A. Ahmad, J. C. Roh *et al.*, "Vital signs monitoring of multiple people using a fmcw millimeter-wave sensor," in *2018 IEEE Radar Conference (RadarConf18)*. IEEE, 2018, pp. 1450–1455.
[10] K. Liu, C. Ding *et al.*, "A coarse-to-fine robust estimation of fmcw radar signal for vital sign detection," in *2020 IEEE Radar Conference (RadarConf20)*. IEEE, 2020, pp. 1–6.
[11] L. Liu, S. Zhang *et al.*, "Non-contact vital signs detection using mm-wave radar during random body movements," in *2021 IEEE 16th Conference on Industrial Electronics and Applications (ICIEA)*. IEEE, 2021, pp. 1244–1249.
[12] Y. Wang, Z. Wang *et al.*, "Vital sign monitoring in dynamic environment via mmwave radar and camera fusion," *IEEE Transactions on Mobile Computing*, 2023.
[13] S. M. Patole, M. Torlak *et al.*, "Automotive radars: A review of signal processing techniques," *IEEE Signal Processing Magazine*, vol. 34, pp. 22–35, 2017. [Online]. Available: https://api.semanticscholar.org/CorpusID:12781159
[14] C. Iovescu, "The fundamentals of millimeter wave sensors," 2017. [Online]. Available: https://api.semanticscholar.org/CorpusID:30625501
[15] Texas Instruments, "Awr1243 boost mmwave sensing solution," Online, 2023, available: https://www.ti.com/product/AWR1243.
[16] M. Alizadeh, G. Shaker *et al.*, "Remote monitoring of human vital signs using mm-wave fmcw radar," *IEEE Access*, vol. 7, pp. 54 958–54 968, 2019.
[17] H. Pan, X. Zhu *et al.*, "Real-time wireless ecg-derived respiration rate estimation using an autoencoder with a dct layer," in *ICASSP 2023-2023 IEEE International Conference on Acoustics, Speech and Signal Processing (ICASSP)*. IEEE, 2023, pp. 1–5.
[18] F. Wang, F. Zhang *et al.*, "Vimo: Multiperson vital sign monitoring using commodity millimeter-wave radio," *IEEE Internet of Things Journal*, vol. 8, no. 3, pp. 1294–1307, 2020.